Journal of Industrial and Engineering Chemistry 88 (2020) 319–327

Contents lists available at ScienceDirect

Journal of Industrial and Engineering Chemistry

journal homepage: www.elsevier.com/locate/jiec

Flow synthesis of polycrystalline ZIF-8 membranes on polyvinylidene fluoride hollow fibers for recovery of hydrogen and propylene

Mohamad Rezi Abdul Hamid[a,*], Hae-Kwon Jeong[b,c,*]

[a] Department of Chemical and Environmental Engineering, Universiti Putra Malaysia, Serdang, Selangor 43400, Malaysia
[b] Artie McFerrin Department of Chemical Engineering, Texas A&M University, College Station, Texas 77843-3122, United States
[c] Department of Materials Science and Engineering, Texas A&M University, College Station, Texas 77843-3122, United States

ARTICLE INFO

Article history:
Received 7 March 2020
Received in revised form 18 April 2020
Accepted 29 April 2020
Available online 12 May 2020

Keywords:
Metal organic frameworks
Zeolitic imidazolate frameworks
Membranes
Hollow fibers
Gas separations

ABSTRACT

It is highly desirable to prepare defect-free ZIF-8 membranes on commercially attractive scalable polymer hollow fibers, especially on the bore side of the fibers, yet quite challenging. Herein, we report a facile synthesis of well-intergrown ZIF-8 membranes on polyvinylidene fluoride (PVDF) microfiltration hollow fibers by a secondary growth method. Surface modification using a strong base promoted high heterogeneous nucleation, resulting in densely packed ZIF-8 seed layers on the hollow fibers. The seed crystals were secondarily grown under a continuous flow of growth solution to form ZIF-8 membranes with thickness of ~1.2 μm. The prepared ZIF-8 membranes achieved high gas permeances, reaching values of $16{,}344 \times 10^{-10}$ mol m^{-2} s^{-1} Pa^{-1} for H_2 and 197×10^{-10} mol m^{-2} s^{-1} Pa^{-1} for C_3H_6. The selectivities for H_2/CH_4, H_2/C_3H_6, H_2/C_3H_8 and C_3H_6/C_3H_8 gas pairs were found to be 12, 57, 160 and 15, respectively. We anticipate that the method could potentially be applied to transform commercial PVDF ultrafiltration/microfiltration hollow fibers commonly used for water separation into high quality ZIF-8 membranes for H_2 purification and C_3H_6/C_3H_8 separation.

Introduction

Zeolitic-imidazolate frameworks (ZIFs) [1,2], an emerging class of porous crystalline materials, have attracted tremendous scientific interest due to their ultramicroporosity (< 5 Å), high surface area, chemical tunability and chemical/thermal stability [3]. Unique properties of ZIFs make them attractive for a broad variety of advanced applications including catalysis, sensing, adsorption and separation [4–9]. ZIFs are comprised of ML_4 tetahedra (where M = divalent metal ions, e.g., Zn^{2+}, Co^{2+}, etc.) bridged by imidazolate-based ligand (L) forming three dimensional structures similar to those of aluminosilicate zeolites [1]. Among the different ZIFs that are available, ZIF-8 with sodalite (SOD) topology has been extensively investigated for gas separation applications. ZIF-8 possess large cavities of 11.6 Å in diameter accessible through six-membered ring apertures of 3.4 Å (crystallographically-defined pore aperture) [10]. Interestingly, linker flexibility of ZIF-8 enlarges its apertures to 4.0–4.2 Å (effective aperture), rendering high resolution separation of H_2 (2.9 Å) or C_3H_6 (4.0 Å) from C_3H_8 (4.2 Å) possible [11,12].

There have been several reports on the synthesis of polycrystalline ZIF-8 membranes for H_2 purification and C_3H_6/C_3H_8 separation. The synthesis routes to prepare polycrystalline ZIF-8 membranes can be broadly classified into two categories: *in-situ* [13–15] growth and secondary growth [16–18]. In general, the synthesis of polycrystalline ZIF-8 membranes via secondary growth is preferred as nucleation and growth of ZIF-8 are decoupled, allowing greater degree of freedom over control of membrane microstructures [19]. A vast majority of polycrystalline ZIF-8 membranes were prepared on inorganic ceramic substrates which are not readily scalable as compared to polymer substrates. On the other hand, polymer hollow fibers are attractive as scalable supports since they are inexpensive and easy to be packed into modules [20]. Hollow fiber modules have surface-to-volume ratio of about 6500–13,000 m^2 m^{-3}, significantly greater than spiral wound modules (650–820 m^2 m^{-3}) and plate and frame modules (320–490 m^2 m^{-3}) [21]. It is noted that hollow fibers with surface-to-volume ratio greater than 1000 m^2 m^{-3} are considered attractive for commercial applications [22]. Polyvinylidene fluoride (PVDF) hollow fibers have been extensively used for water and wastewater treatment as microfiltration or ultrafiltration hollow fiber membranes and currently explored for bio-separation

* Corresponding authors.
E-mail addresses: mohamadreziabdulhamid89@gmail.com (M.R. Abdul Hamid), hjeong7@tamu.edu (H.-K. Jeong).

https://doi.org/10.1016/j.jiec.2020.04.031
1226-086X/

applications [23]. Porous PVDF hollow fibers can be prepared via phase inversion method, which is a simple and frequently used method in large scale membrane production [24].

There are only a handful of ZIF-8 membranes supported on PVDF hollow fibers. This is primarily due to inertness of PVDF which leads to poor heterogeneous nucleation of ZIF-8 [25]. To enhance heterogeneous nucleation of ZIF-8 on the PVDF supports, physical/chemical functionalization steps were often introduced [26–28]. Li et al. [15,29] coated zinc oxide sol-gel thin films on the shell side of PVDF hollow fibers which were then converted to ZIF-8 membranes in the presence of linker vapors. The resulting ZIF-8 membranes with thickness of ~0.087 μm showed impressive C_3H_6 permeance and separation factor of 2800×10^{-10} mol m^{-2} s^{-1} Pa^{-1} and 73, respectively. Hou and co-workers [26,28] fabricated ~1.0 μm thick ZIF-8 membranes on the shell of PVDF hollow fibers for H_2/CO_2 separation. The hollow fibers were functionalized with APTES-titania to promote heterogeneous crystallization of ZIF-8 on the surface. Li et al. [27] introduced ammonization-based chemical modifications on PVDF hollow fibers to prepare continuous ZIF-8 membranes for H_2 separation.

Despite a few laboratory scale successes [15,29–31], transitioning from planar supports to hollow fiber supports for the synthesis of ZIF-8 membranes still remains challenging. This is primarily due to the lack of understanding of ZIF-8 membrane formation on the inner surface of a confined space, such as in the case of polymer hollow fibers, using continuous flow processing. From our previous experience with the synthesis of ZIF-8 membranes on Matrimid® 5218 hollow fibers using microfluidic secondary growth [30–32], we attempted to extend the work to prepare ZIF-8 membranes on PVDF hollow fibers since PVDF hollow fibers are cheaper and more readily available than imide-based hollow fibers. In the present work, we first introduced a new ZIF-8 seeding process which is based on dehydrofluorination reaction to promote the formation of ZIF-8 seed nanocrystals on the bore side of the hollow fibers. Second, we investigated important processing parameters (e.g., base treatment time and secondary growth flow rate) in order to obtain thin and compact ZIF-8 membranes on the hollow fibers. Finally, we assessed the gas separation properties of the membranes focusing primarily on H_2 purification and C_3H_6/C_3H_8 separation.

Experimental

Materials

A PVDF hollow fiber microfiltration membrane module (Microza® UMP-1047R) was purchased from Pall Corporation. Potassium hydroxide (KOH, reagent grade, VWR International) was used to chemically modify the PVDF hollow fibers. Zinc nitrate hexahydrate ($Zn(NO_3)_2.6H_2O$, 98%, Sigma-Aldrich), 2-methylimidazole (hereafter MeIM, $C_4H_6N_2$, 99%, Sigma-Aldrich), sodium formate (HCOONa, 99%, Sigma-Aldrich), methanol (CH_3OH, > 99%, Alfa-Aesar) and deionized water were used as precursors to prepare ZIF-8 seed layers and membranes. Polydimethylsiloxane (PDMS, Sylgard® 184 Silicone Elastomer Kit, Sigma-Aldrich) and hexane (C_6H_{14}, ACS grade, VWR International) were used to seal ZIF-8 membrane defects. Ethanol (C_2H_5OH, 94–96%, Alfa-Aesar) was used as solvent to clean the PVDF hollow fibers.

Preparation of PVDF hollow fibers and synthesis setup

The membrane module was first disassembled to obtain individual PVDF hollow fibers (see Fig. S1). The PVDF hollow fibers have inner and outer diameter (ID and OD) of 1.4 mm and 2.2 mm, respectively. The hollow fibers were then immersed in ethanol at room temperature overnight to remove glycerin preservative from pores of the hollow fibers. Then, the hollow fibers were dried in a convection oven at 60 °C overnight to remove the ethanol solvent. A custom-made synthesis setup containing a hollow fiber was prepared according to the procedure reported elsewhere [30]. In brief, a PVDF hollow fiber 100 mm in length was inserted into a Teflon® tubing (ID 4.76 mm and OD 6.35 mm) having a similar length. The main function of the Teflon® tubing is to provide handling convenience during ZIF-8 membrane synthesis. The shell side of PVDF hollow fiber was properly sealed with an epoxy resin (Devcon® 2 Ton Epoxy) and the epoxy was allowed to cure at room temperature for 24 h. Excess PVDF ends were carefully removed using a razor blade. Digital photograph of the synthesis setup is shown in Fig. S2.

Preparation of ZIF-8 seed layers

ZIF-8 seed layers on the bore side of the hollow fiber (hereafter, PVDF-X-S) were synthesized following the procedure described elsewhere [30]. An aqueous KOH solution was used to modify PVDF polymer. Using a syringe pump (Harvard Model 55–4152), a warm (50 °C) KOH solution (5.0 mol L^{-1}) was fed to the bore side of the hollow fiber at a flow rate of 0.33 mL min^{-1} for different period of time. The KOH-treated PVDF hollow fiber (hereafter, PVDF-X, where X represents the KOH treatment time in min) was then saturated with an aqueous Zn solution (0.1 mol L^{-1}) at a flow rate of 0.33 mL min^{-1} for 1 h (hereafter, PVDF-X-Zn). Excess KOH and Zn solutions were manually purged with air and dried with Kimwipes. Then, the Zn-saturated hollow fiber was positioned vertically inside a Teflon® autoclave containing a ligand solution (10.36 g of MeIM and 0.5 g sodium formate in 120 mL of methanol). Immediately after, the autoclave was kept inside a preheated convection oven at 120 °C for 1 h. After the solvothermal reaction, the autoclave was naturally cooled down to room temperature for 2 h. Finally, the seeded hollow fiber was washed with methanol for 1 h and then dried in an oven at 60 °C overnight.

Preparation of ZIF-8 membranes

ZIF-8 seed layers on PVDF hollow fiber (i.e., PVDF-X-S) were subjected to a continuous flow of secondary growth solution at room temperature for 6 h to obtain a well-intergrown ZIF-8 membrane (hereafter, PVDF-X-M). Secondary growth flow rate was manipulated to obtain ZIF-8 membrane with desired thickness and separation performance. Grain boundary defects of ZIF-8 membrane can be minimized by coating a thin layer of PDMS on top of the membrane (hereafter, PVDF-X-M-PDMS). General procedures to prepare a secondary growth precursor solution and a dilute PDMS solution can be found elsewhere [30,31]. In brief, a secondary growth precursor solution was prepared by mixing metal (0.11 g of zinc nitrate hexahydrate in 20 mL of deionized water) and linker (2.27 g of MeIM in 20 mL of deionized water) precursor solutions at room temperature for 1 min. Immediately after, the secondary growth solution was loaded into a polypropylene syringe and then properly secured on a syringe pump (see Fig. S2). After secondary growth has completed, the hollow fiber was washed by flowing fresh methanol through the hollow fiber at a flow rate of 0.33 mL min^{-1} for 1 h. The hollow fiber was then dried at room temperature for 24 h. On the other hand, a dilute (10 wt%) PDMS solution was prepared by mixing Part A and Part B (10:1 ratio) of PDMS in hexane. The solution is vigorously mixed at room temperature for several hours prior to use. PDMS coating was performed by flowing PDMS solution through the bore side of the hollow fiber at a flow rate of 0.11 mL min^{-1} for 1 min. Excess PDMS solution trapped inside the hollow fiber was carefully purged by flowing air at a flow rate of 0.33 mL min^{-1} for 1 min. Finally, the

PDMS-coated ZIF-8 membrane was dried at room temperature under vacuum for 48 h.

Characterization and gas permeation test

Attenuated total reflection Fourier transform infrared (ATR-FTIR) spectra were taken using a Nicolet FTIR (iS5, Thermo Scientific) equipped with iD7-ATR diamond. Powder X-ray diffraction (XRD) patterns were collected using a Rigaku Miniflex II X-ray diffractometer (Cu-Kα radiation and 2θ scan range of 5–25°). Electron micrographs were obtained using a JEOL JSM-7500 F (acceleration voltage of 5 keV and working distance of 15 mm). H_2, CO_2, N_2, CH_4, C_3H_6 and C_3H_8 single gas permeations through ZIF-8 membranes were performed using a Wicke-Kallenbach technique shown in Fig. S3. On the other hand, binary gas permeation measurements were carried out using an equimolar (1:1) mixture of C_3H_6 and C_3H_8 as feed gas. Flow rates of feed and argon sweep gases were set at 50 $cm^3\,min^{-1}$. The permeation measurements (single and binary) were performed at room temperature under atmospheric pressure. Compositions of gases permeated through the ZIF-8 membranes were analyzed using mass spectrometer (QGA Hiden Analytical) and gas chromatography (Agilent GC 7890 A).

Gas permeance of component i, F_i, is defined as (1):

$$F_i = \frac{N_i}{A \times \Delta P_i} \quad (1)$$

where, N_i is molar flow rate of component i (mol s^{-1}), ΔP_i is partial pressure difference of component i across the membrane (Pa) and A is membrane area (m^2).

Ideal selectivity ($\alpha_{i/j}$) is defined as the ratio of permeability or permeance of individual gas (2).

$$\alpha_{i/j} = \frac{F_i}{F_i} \quad (2)$$

For binary mixture, separation factor ($\alpha_{i/j}$) is defined as (3):

$$\alpha_{i/j} = \frac{F_i}{F_j} = \frac{\frac{y_i}{y_j}}{\frac{x_i}{x_j}} \quad (3)$$

where, x_i and x_j are the molar fraction of component i and j at feed side, respectively, and y_i and y_j are the molar fraction of component i and j at permeate side, respectively.

Result and discussion

Characterization of each synthesis step

A key concept behind this method is to modify the relatively inert PVDF polymer using a strong base to create abundant active surface groups which promotes heterogeneous nucleation of ZIF-8. As depicted in Scheme 1 chemical reactions between PVDF hollow fibers and a strong base (KOH) led to elimination of hydrogen fluoride groups (commonly referred as PVDF dehydrofluorination) and formation of carbon-carbon double bonds (C=C) and hydroxyl bonds (−OH) [24,33]. High quality ZIF-8 seed layers were obtained by solvothermally treating the Zn-saturated PVDF hollow fibers in a ligand solution. Hydroxyl groups on hollow fiber surfaces chelate with Zn ions to promote heterogeneous nucleation, thereby resulting in densely packed ZIF-8 seed layers with uniform surface coverage [34]. In addition, surface hydroxyl groups of the modified PVDF can form coordination bonds with ZIF-8 to create strongly adhered ZIF-8 layers on the substrates, hence improving their mechanical stability [35]. It is worthy of mentioning that the location of ZIF-8 seed layers can be controlled by simply flowing the KOH solution on a preferred surface (i.e., bore side vs. shell side) of the hollow fibers. Finally, the ZIF-8 seed nanocrystals were secondarily grown to form well-intergrown and compact ZIF-8 membranes following a similar procedure previously reported [30].

Individual PVDF hollow fibers disassembled from a membrane module have ID and OD of 1.4 mm and 2.2 mm, respectively. The calculated surface-to-volume ratio of the hollow fibers was around 1800 $m^2\,m^{-3}$. As shown in Fig. S4, pore sizes of pristine hollow fibers were irregular. Pore sizes as large as 0.8 μm in diameter were also observed. Fig. 1(a–b) shows the ATR-FTIR spectra of unmodified (PVDF), KOH-treated (PVDF-9) and Zn-saturated (PVDF-9-Zn) hollow fibers. Characteristic IR peaks of pristine PVDF at 872 cm^{-1}, 1182 cm^{-1} and 1404 cm^{-1} can be ascribed to the stretching vibration of C—C, —CF_2 and —CH_2, respectively [36]. After 9 min of KOH treatment (i.e., PVDF-9) followed by 1 h of Zn saturation (i.e., PVDF-9-Zn), two new IR peaks assigned to C=C (1640 cm^{-1}) and −OH (3000–3400 cm^{-1}) bonds were observed, indicating modification of PVDF upon dehydrofluorination reaction (see Fig. 1(c)) [37,38]. XRD patterns of the samples presented in Fig. S5(a) were more or less identical. The two major diffraction peaks at 2θ values of

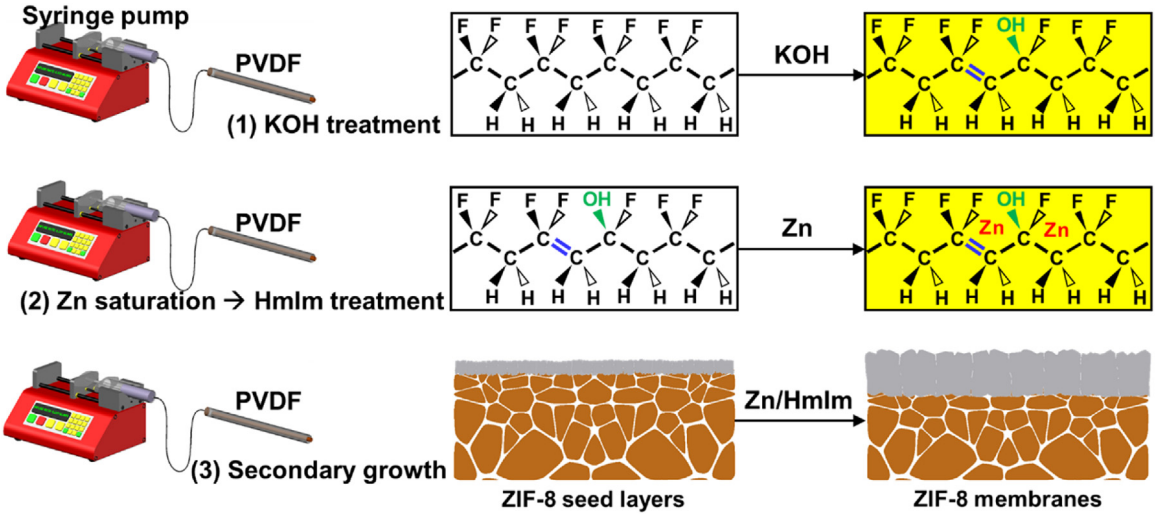

Scheme 1. Schematic illustration of the synthesis of ZIF-8 membranes on the bore side of PVDF hollow fibers via secondary growth.

19° and 21° were assigned to α and β-phases of the PVDF, respectively [39]. Furthermore, scanning electron micrographs (SEM) of the samples in Fig. S5(b–d) showed no noticeable changes in the PVDF surface morphology. These results strongly suggests that dehydrofluorination reaction does not compromise the long-range orders and microstructures of PVDF substrates.

Microstructure control of ZIF-8 seed layers and membranes

ZIF-8 seed crystals were prepared by solvothermally treating the Zn-saturated PVDF hollow fibers (PVDF-9-Zn) in a linker solution. Fig. 2 presents XRD patterns, IR spectra and SEM images of the ZIF-8 seed layers. The XRD peaks, albeit weak, were consistent with a simulated pattern of ZIF-8, confirming the

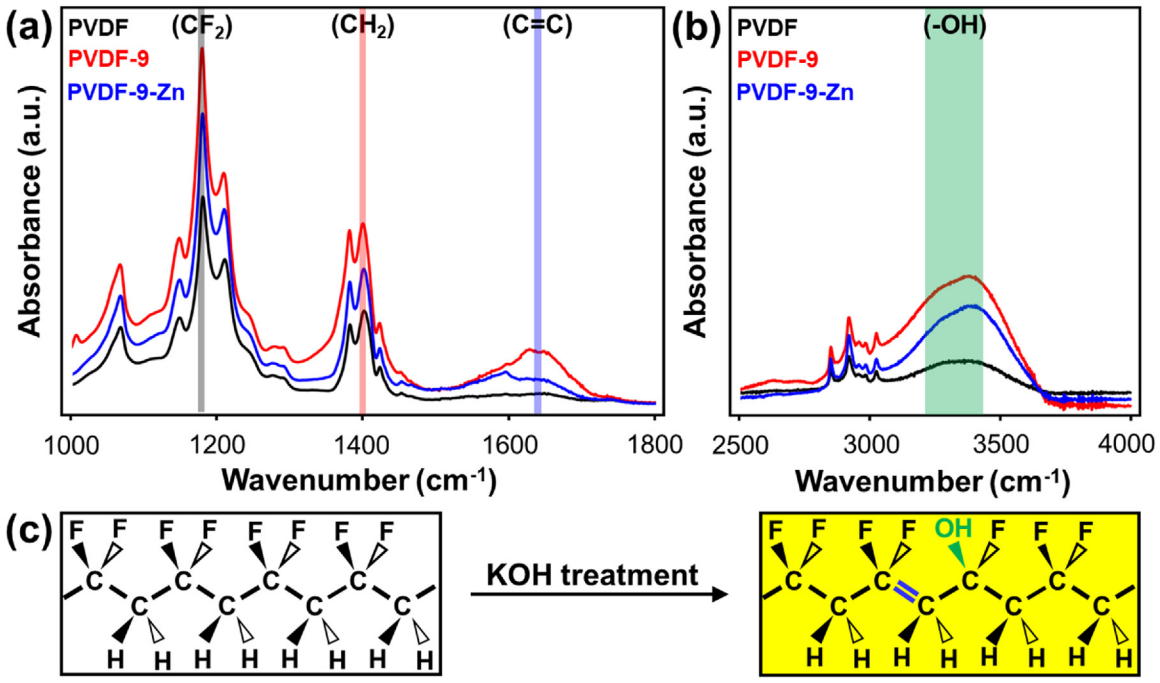

Fig. 1. (a–b) ATR-FTIR spectra of pristine (PVDF), 9 min KOH-treated (PVDF-9) and Zn-saturated (PVDF-9-Zn) hollow fibers. (c) Illustration of PVDF dehydrofluorination by KOH.

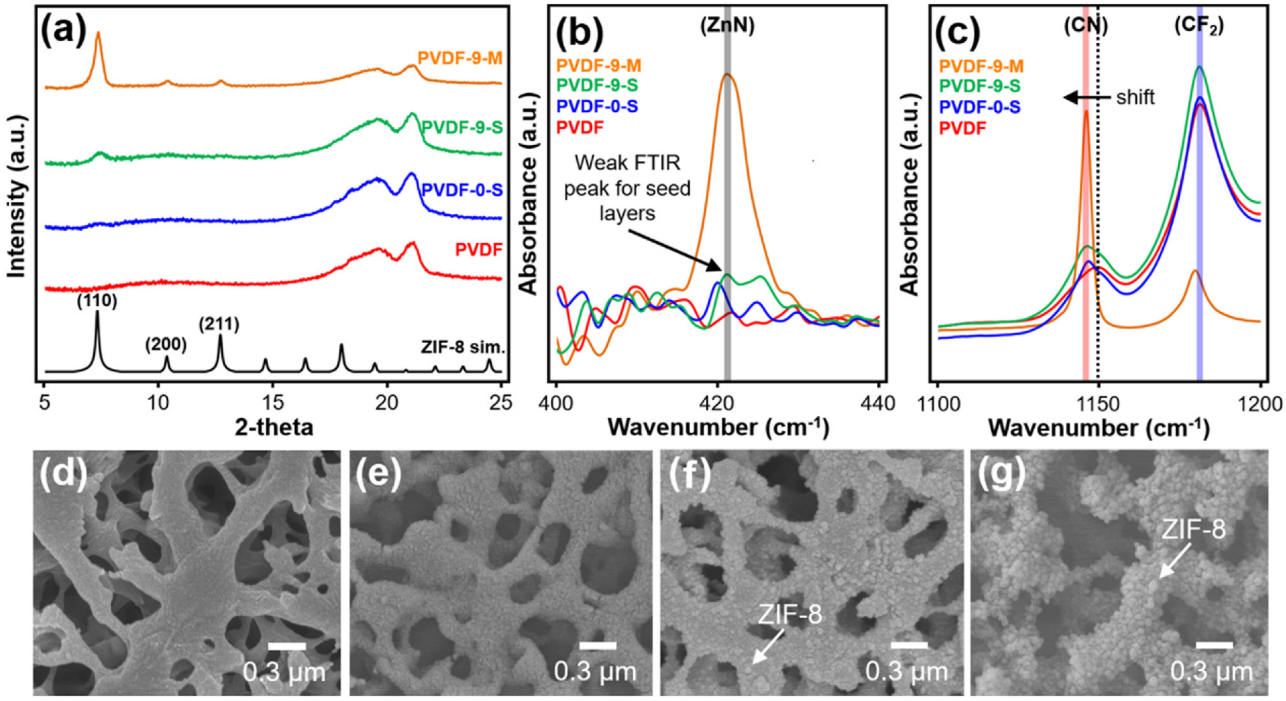

Fig. 2. (a) XRD patterns and (b–c) ATR-FTIR spectra of pristine hollow fibers (PVDF), ZIF-8 seed layers deposited on PVDF hollow fibers with (PVDF-9-S) and without (PVDF-0-S) KOH treatment and ZIF-8 membranes after secondary growth (PVDF-9-M). Top SEM images of (d) pristine hollow fibers and ZIF-8 seed layers on PVDF hollow fibers treated in KOH for (e) 0 min (f) 9 min and (g) 20 min.

formation of pure phase SOD-ZIF-8 seed crystals. In addition, characteristic IR bands of ZIF-8 at 421 cm^{-1} (Zn–N) and 1145 cm^{-1} (C–N) were observed [30]. However, the IR peaks of the seeded hollow fibers were low in intensity that sometimes indistinguishable from the peaks of pristine fibers partly due to the lack of access into the bore of the hollow fibers for proper IR characterization. SEM images of the seeded hollow fibers in Fig. 2(f) showed the presence of ZIF-8 seed crystals with an average particle size of around 60 nm uniformly covering the hollow fiber surfaces. No seed crystals were observed on the shell side of the hollow fibers, indicating that the majority of the seed crystals are grown selectively on the bore side of the hollow fibers (see Fig. S6).

A control experiment was performed to highlight the importance of KOH treatment to obtain densely packed ZIF-8 seed layers on PVDF substrates. As shown in Fig. 2(e), without KOH treatment (i.e., PVDF-0-S), very few ZIF-8 seed nanocrystals formed on hollow fiber surfaces. The SEM observation was consistent with the XRD and IR results shown in Fig. 2(a–b). This is in stark contrast to the ZIF-8 seed layers prepared using 9 min of KOH treatment (i.e., PVDF-9-S), attributable to the lack of surface hydroxyl groups available on the hollow fiber surfaces. In other words, intrinsic surface properties of pristine PVDF hollow fibers are not desirable for heterogeneous nucleation of ZIF-8. The results therefore highlight the importance of dehydrofluorination reaction by KOH to obtain high density ZIF-8 seed layers. Attempts to obtain greater number of ZIF-8 seed layers (by increasing KOH treatment time to 20 min) were unsuccessful as further degradation of polymer chains coupled with excessive loss of fluorine atoms resulted in surface pore enlargements, compromising the microstructures of the PVDF substrates [40]. As shown in Fig. 2(g), even though the number of ZIF-8 seed crystals increased, enlarged and more disconnected pores may affect the quality of the ZIF-8 membranes (see also Fig. S7). After carefully analyzing the seed layer microstructures of each samples, a 9 min KOH treatment time was selected as the optimized condition to prepare densely packed ZIF-8 seed layers.

ZIF-8 seed layers (PVDF-9-S) were secondarily grown under a continuous flow of growth solution to obtain compact and well-intergrown membranes. As shown in Fig. 2(a–c), the ZIF-8 membranes after secondary growth (PVDF-9-M) displayed stronger XRD and IR peak intensities as compared to the ZIF-8 seed layers, suggesting growth of the seed crystals. It is worthy of mentioning that ZIF-8 membranes prepared using poor quality seed layers (i.e., PVDF-0-M and PVDF-20-M) did not exhibit high separation performances. The secondary growth flow rate was appropriately manipulated to obtain ZIF-8 membranes with optimized microstructures. The secondary growth of ZIF-8 seed crystals was initially carried out at a flow rate of 0.01 mL min^{-1} and later increased to 0.05 mL min^{-1} and 0.10 mL min^{-1} while maintaining secondary growth time fixed at 6 h. As shown in Fig. 3, higher secondary growth flow rate produced better intergrown membranes with larger grain sizes. Moreover, thickness of the ZIF-8 membranes increased from 0.3 μm to 1.2 μm. Precursor concentration at the vicinity of seed crystals is higher at higher secondary growth flow rate, which in turn promotes crystal growth (i.e., thicker films). Based on careful microstructure analysis, secondary growth flow rate of 0.10 mL min^{-1} was chosen as an optimized condition since the resulting membranes were more intergrown, thereby likely to be less defective. In fact, among ZIF-8 membranes that were synthesized, the membranes prepared using secondary growth flow rate of 0.10 mL min^{-1} showed the most promising separation performances (will be discussed in later section).

H_2 separation performances of ZIF-8 membranes

Separation performances of the prepared ZIF-8 membranes were assessed by measuring permeances of gases with different kinetic diameters. Single gas permeances of H_2, CO_2, N_2, CH_4, C_3H_6 and C_3H_8 were measured using the Wicke-Kallenbach technique (Fig. S3). It is noted that ZIF-8 membrane module has an active membrane length of 40 mm (active membrane area of 176 mm^2). The gas permeances and ideal selectivities of the ZIF-8 membranes are presented in Fig. 4. The ZIF-8 membranes displayed high H_2 permeance, reaching value of 16,344 × 10^{-10} mol m^{-2} s^{-1} Pa^{-1} (4882 GPU), which is much higher than those of other gases. The measured gas permeances through ZIF-8 membranes proceed following the order of molecule kinetic diameters (H_2 > CO_2 > N_2 > CH_4 > C_3H_6 > C_3H_8), suggesting that separations between H_2 and larger gases through the membranes were based on molecular

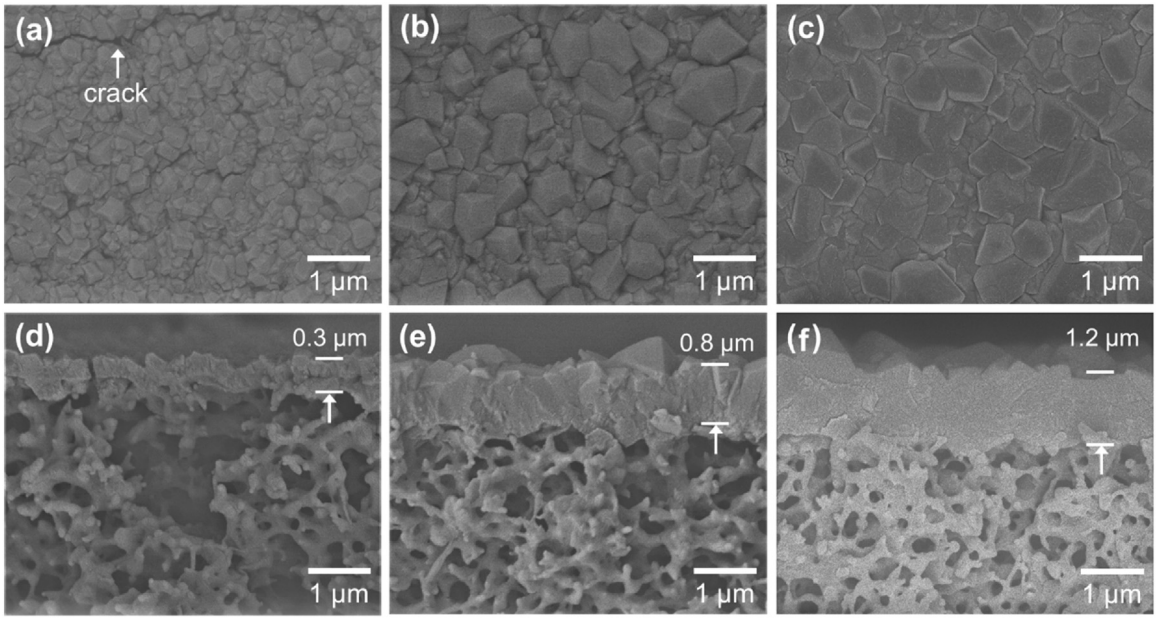

Fig. 3. (a–c) Top and (d–f) cross-sectional SEM images of ZIF-8 membranes synthesized using different secondary growth flow rates: 0.01 mL min^{-1}, 0.05 mL min^{-1} and 0.10 mL min^{-1}.

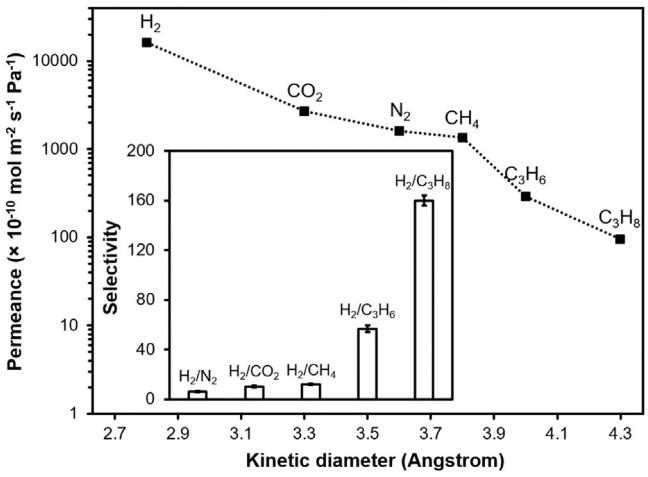

Fig. 4. Single gas permeances of ZIF-8 membranes supported on PVDF hollow fibers as a function of molecule kinetic diameters. Note that the ZIF-8 membranes (i.e., PVDF-9-M) were synthesized using secondary growth flow rates of 0.10 mL min^{-1}.

sieving mechanism. No sharp cut off exist at 3.4 Å (nominal pore aperture of ZIF-8) due to flexibility of ZIF-8 frameworks which allows molecules greater than 3.4 Å (e.g., N_2 – 3.6 Å and CH_4 – 3.8 Å) to diffuse through the membranes [41]. This observation is in agreement with other reports [16,42]. Ideal selectivities for H_2/CO_2, H_2/N_2, H_2/CH_4, H_2/C_3H_6 and H_2/C_3H_8 gas pairs were determined to be 6.0, 10.2, 12.1, 56.6 and 160.1, respectively, which are higher than the corresponding the Knudsen constants (4.7, 3.7, 2.8, 4.6, and 4.7). As shown in Fig. S8, H_2 permeances and ideal selectivities of the ZIF-8 membranes easily surpassed the Robeson upper bound of 2008. The separation performances also compares favorably with those reported in the literatures (Table 1).

C_3H_6/C_3H_8 separation performances of ZIF-8 membranes

ZIF-8 is well-known for having high C_3H_6/C_3H_8 separation properties due to its well-fitted effective pore apertures of 4.0–4.2 Å. This enables a high resolution separation of C_3H_6 (4.0 Å) from C_3H_8 (4.2 Å) based on molecular sieving mechanism [11,12]. For example, polycrystalline ZIF-8 membranes supported on inorganic substrates with the C_3H_6/C_3H_8 separation factor greater than 100 have been reported [29,51–55]. Binary C_3H_6/C_3H_8 permeation measurements of ZIF-8 membranes were performed using Wicke-Kallenbach technique. As shown in Fig. S3, an equimolar (1:1) mixture of C_3H_6 and C_3H_8 was provided through the bore side of the hollow fibers while argon sweeping gas was provided through the shell side of the hollow fibers. The composition of gases permeated through the membranes were measured using gas chromatography.

It is important to note that the pristine PVDF hollow fibers were not selective towards C_3H_6 and exhibited high C_3H_6 permeance of 4992×10^{-10} mol m^{-2} s^{-1} Pa^{-1}. Binary C_3H_6/C_3H_8 separation performances of ZIF-8 membranes fabricated using different secondary growth flow rates are presented in Table 2. ZIF-8 membranes synthesized using secondary growth flow rate of 0.01 mL min^{-1} have high C_3H_6 permeance (4341×10^{-10} mol m^{-2} s^{-1} Pa^{-1}) and does not exhibit molecular sieving property possibly due to formation of macroscopic defects such as cracks and pinholes. SEM images in Fig. 3(a) confirmed that macroscopic defects (i.e., cracks) exist on the membrane surfaces which compromise separation performances of the membranes. ZIF-8 membranes grown using secondary growth flow rate of 0.10 mL min^{-1} on the other hand exhibited lower C_3H_6 permeance (275×10^{-10} mol m^{-2} s^{-1} Pa^{-1}), but improved C_3H_6/C_3H_8 separation factor (3.0) attributable to a thicker membrane layer with better intergrowth. The current separation performances of the prepared ZIF-8 membranes however are not attractive for industrial applications.

Polycrystalline membranes, including ZIF-8 membranes, by their very nature will always contain grain boundaries with channel diameters larger than the six-membered ring apertures of ZIF-8 (3.4 Å) [56]. As illustrated in Fig. 5(f), gas transports through ZIF-8 membranes are governed by the diffusion through crystal grains (intrinsically selective diffusion pathway) and through crystal grain boundaries (non-selective diffusion pathway) [57]. Large molecules such as C_3H_8 (4.2 Å) may be able to diffuse through these non-selective inter-crystalline gaps, resulting in lower C_3H_6/C_3H_8 separation efficiency.

It is surmised that the ZIF-8 membranes reported in this work possess poor grain boundary structures likely due to PVDF large pore sizes. The nature of substrates including pore sizes, surface roughness and chemical composition can affect the microstructures of the ZIF-8 layers [9]. As previously mentioned, the PVDF hollow fibers used in this study have large and irregular sized pores. Pores as large as 1.2 μm in diameter were even observed under electron microscope. Even though densely packed ZIF-8 seed layers were successfully grown on the support surfaces, in order to form continuous ZIF-8 layers, these seed crystals must grow and cover these large pores, likely leading to poor grain boundary structures. Note that this phenomenon is not unique to our work. For instance, Li and co-workers reported that they were also unable to synthesize high quality ZIF-8 membranes on Al_2O_3 tubes due to substrate large pore sizes [58].

Table 1
Comparison of H_2 permeances and selectivities reported in this work with those reported in the literatures.

Substrate	Location	Thickness (μm)	H_2 Permeance[a]	Selectivity			Ref
				H_2/CO_2	H_2/N_2	H_2/CH_4	
PVDF hollow fiber	Bore	1.2	15,890	12.0	6.3	13.6	This work
PVDF hollow fiber	Shell	1.1	175,000	7.3	6.3	5.0	[28]
PVDF hollow fiber	Shell	30	24,430	12.2	14.3	–	[27]
Polysulfone hollow fiber	Bore	3.6	48	2.6	18.3	17.2	[22]
ZnO-Al_2O_3 hollow fiber	Shell	5.0	18,100	6.0	10.4	11.7	[43]
Al_2O_3 hollow fiber	Shell	20	7290	5.4	9.2	10.8	[44]
Al_2O_3 hollow fiber	Shell	5.0	11,000	5.2	7.3	6.8	[45]
Al_2O_3 hollow fiber	Bore	2.0	4324	3.3	11.1	12.1	[46]
Al_2O_3 tube	Bore	5.0	1030	12.8	24.2	40.1	[47]
Al_2O_3 disc	–	20	2170	10.3	17.6	34.8	[48]
AAO disc	–	0.8	47,140	12.5	3.6	9.8	[49]
BPPO disc	–	2.0	6000	9.0	5.5	10.0	[50]
Titania disc	–	42	674	8.2	4.1	11.2	[42]

[a] Permeance unit: $\times 10^{-10}$ mol m^{-2} s^{-1} Pa^{-1}.

Table 2
Binary C_3H_6/C_3H_8 separation performances of ZIF-8 membranes on PVDF hollow fibers.

Secondary growth flow rates (ml min^{-1})	Permeance ($\times 10^{-10}$ mol m^{-2} s^{-1} Pa^{-1})		Separation factor
	C_3H_6	C_3H_8	
Pristine	4992 ± 38	5677 ± 65	0.9 ± 0.0
0.01	4341 ± 122	4890 ± 283	1.0 ± 0.0
0.05	516 ± 30	336 ± 9	1.5 ± 0.1
0.10	275 ± 19	108 ± 6	3.1 ± 0.7
0.10 (with PDMS)	197 ± 2	13 ± 2	15 ± 2.8

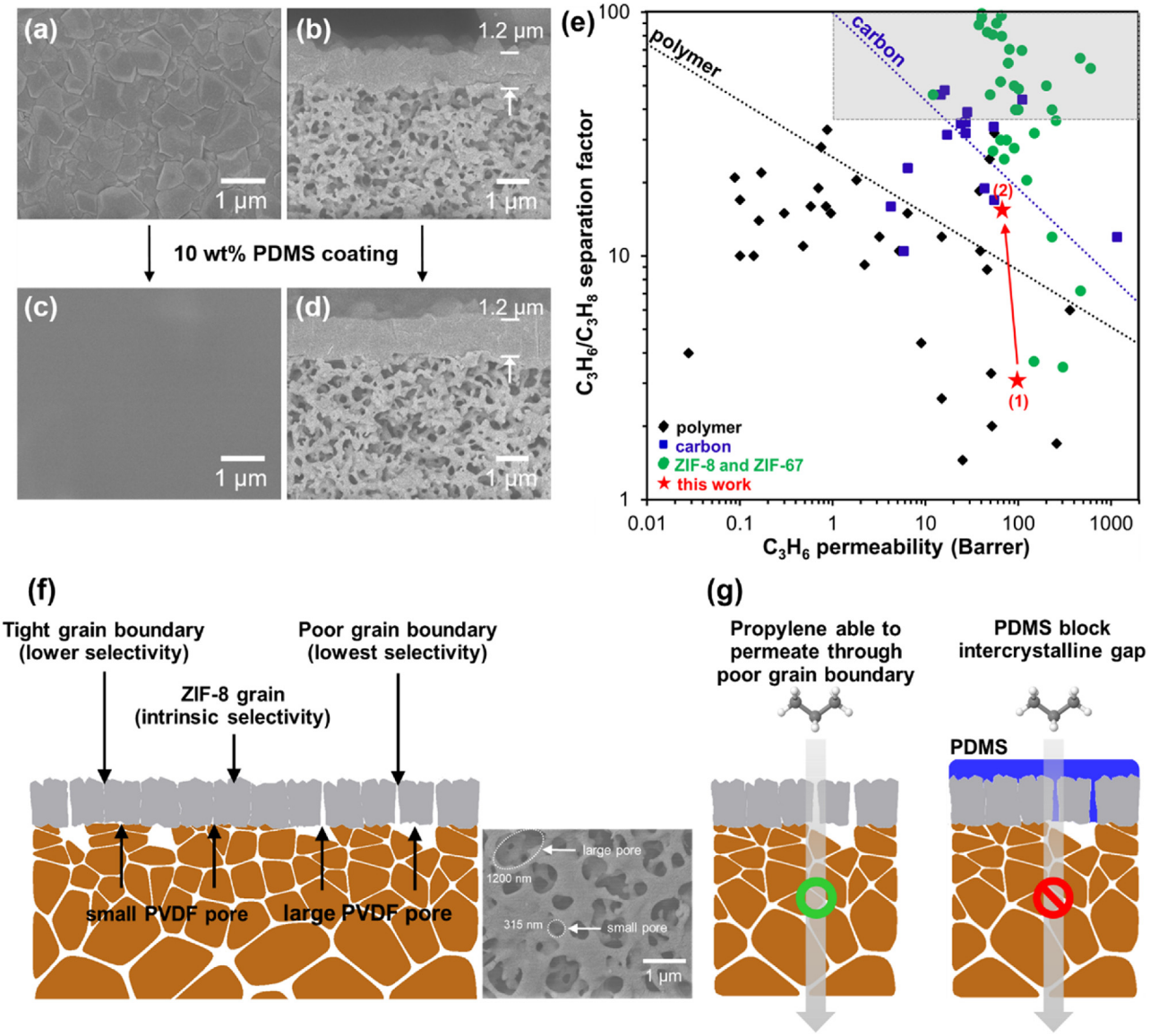

Fig. 5. Top and cross-sectional SEM images of (a–b) PVDF-9-M and (c–d) PVDF-9-M-PDMS. (e) Binary C_3H_6/C_3H_8 separation performances of PVDF-9-M (1) and PVDF-9-M-PDMS (2) compared to those reported in literatures which include ZIF-8 and ZIF-67 membranes supported on inorganic substrates (discs [14,17,18,34,57,59–71], tubes [58,72,73] and hollow fibers [52,74]) and polymer substrates (flat sheets [50,75] and hollow fibers [13,15,30–32,76,77]). Illustration of (f) ZIF-8 membrane grain boundary structures across small and large PVDF pores and (g) PDMS coating over ZIF-8 layer to block inter-crystalline gaps. Note that the inter-crystalline gaps were exaggerated for illustration purposes.

A common engineering practice to minimize membrane grain boundary defects is through caulking technique [78]. As shown in Fig. 5(g), a thin layer of a highly permeable material (e.g., PDMS) is coated on the ZIF-8 membrane. PDMS has high C_3H_6 permeability of 2400 Barrer but not selective towards C_3H_6 [79]. A sufficiently thin PDMS layer deposited on top of the ZIF-8 membrane will not significantly affect C_3H_6 flux of the membrane. Penetration of PDMS into the inter-crystalline region of ZIF-8 prevents the convective flow or Knudsen flow through these channels resulting in a sharp increase in C_3H_6/C_3H_8 separation factor [57,58]. In addition, hydrophobic PDMS coating provides high water repellency which improves water stability of the membranes [80–84].

PDMS coating of ZIF-8 membranes was performed flowing a dilute PDMS solution through the bore side of the hollow fibers [57]. It is noted that defect abatement of the ZIF-8 membranes was performed without disassembling the membranes from the test modules. Fig. 5(c–d) exhibits a smooth, uniform and thin PDMS coating layer. Upon PDMS coating, though marginal, the C_3H_6/C_3H_8 separation performances were enhanced with C_3H_6 permeance and separation factor of 197×10^{-10} mol m^{-2} s^{-1} Pa^{-1} (59 GPU) and 15, respectively. Even though the performances of our ZIF-8 membranes fell short of the commercially attractive region, our ZIF-8 membranes still have the potential to be retrofitted as membrane/distillation debottlenecking system or as C_3H_6 recovery unit in reactor purge streams as proposed by Freeman and co-workers (required C_3H_6 permeance and separation factor of 50–100 GPU and 5–10, respectively) [85].

Conclusion

We presented a new synthesis strategy to fabricate ZIF-8 membranes on relatively cheap PVDF hollow fiber microfiltration membranes for H_2 purification and C_3H_6/C_3H_8 separation. Densely packed ZIF-8 seed layers on the bore side of PVDF hollow fibers were secondarily grown into ZIF-8 membranes using continuous flow system. The ~1.2 μm thick ZIF-8 membranes displayed a promisingly high H_2 permeance of $16{,}344 \times 10^{-10}$ mol m^{-2} s^{-1} Pa^{-1} and H_2/CH_4, H_2/C_3H_6 and H_2/C_3H_8 ideal selectivities of 12, 57 and 160, respectively. The membranes however did not perform as expected for C_3H_6/C_3H_8 mixture even after PDMS coating step, suggesting poor grain boundary structures. C_3H_6/C_3H_8 separation performances of the membranes can be further improved by optimizing membrane processing. Overall, the method described here is simple and cost-effective, therefore holds promise for scale up. The cost of ZIF-8 membrane on polymeric substrates may not be as cheap as compared to polymeric membranes, but it is definitely more attractive than those grown on inorganic substrates.

Declaration of interests

The authors declare that they have no known competing financial interests or personal relationships that could have appeared to influence the work reported in this paper.

Acknowledgements

The authors acknowledge the financial supports by the National Science Foundation (CBET-1510530 and DBI-0116835), the Qatar National Research Fund (NRRP grant #8-001-2-001), the VP for Research Office and the Texas A&M Engineering Experimental Station.

Appendix A. Supplementary data

Supplementary material related to this article can be found, in the online version, at doi:https://doi.org/10.1016/j.jiec.2020.04.031.

References

[1] K.S. Park, Z. Ni, A.P. Côté, J.Y. Choi, R. Huang, F.J. Uribe-Romo, H.K. Chae, M. O'Keeffe, O.M. Yaghi, Proc. Natl. Acad. Sci. 103 (2006) 10186, doi:http://dx.doi.org/10.1073/pnas.0602439103.
[2] B. Wang, A.P. Côté, H. Furukawa, M. O'Keeffe, O.M. Yaghi, Nature 453 (2008) 207, doi:http://dx.doi.org/10.1038/nature06900.
[3] Y.V. Kaneti, S. Dutta, M.S.A. Hossain, M.J.A. Shiddiky, K.L. Tung, F.K. Shieh, C.K. Tsung, K.C.W. Wu, Y. Yamauchi, Adv. Mater. 29 (2017) 1700213, doi:http://dx.doi.org/10.1002/adma.201700213.
[4] Y.H. Deng, J.T. Chen, C.H. Chang, K.S. Liao, K.L. Tung, W.E. Price, Y. Yamauchi, K.C. W. Wu, Angew. Chem. Int. Ed 55 (2016) 12793, doi:http://dx.doi.org/10.1002/anie.201607014.
[5] M. Vinu, D.S. Raja, Y.C. Jiang, T.Y. Liu, Y.Y. Xie, Y.F. Lin, C.C. Yang, C.H. Lin, S.M. Alshehri, T. Ahamad, J. Taiwan, Inst. Chem. Eng. 83 (2018) 143, doi:http://dx.doi.org/10.1016/j.jtice.2017.11.007.
[6] Y.C. Sue, J.W. Wu, S.E. Chung, C.H. Kang, K.L. Tung, K.C.W. Wu, F.K. Shieh, ACS Appl. Mater. Interfaces 6 (2014) 5192, doi:http://dx.doi.org/10.1021/am5004188.
[7] F.K. Shieh, S.C. Wang, C.I. Yen, C.C. Wu, S. Dutta, L.Y. Chou, J.V. Morabito, P. Hu, M.H. Hsu, K.C.W. Wu, J. Am. Chem. Soc. 137 (2015) 4276, doi:http://dx.doi.org/10.1021/ja513058h.
[8] B. Chen, Z. Yang, Y. Zhu, Y. Xia, J. Mater. Chem. A 2 (2014) 16811, doi:http://dx.doi.org/10.1039/C4TA02984D.
[9] J. Yao, H. Wang, Chem. Soc. Rev. 43 (2014) 4470, doi:http://dx.doi.org/10.1039/C3CS60480B.
[10] X. Gong, Y. Wang, T. Kuang, ACS Sustain. Chem. Eng. 5 (2017) 11204, doi:http://dx.doi.org/10.1021/acssuschemeng.7b03613.
[11] K. Li, D.H. Olson, J. Seidel, T.J. Emge, H. Gong, H. Zeng, J. Li, J. Am. Chem. Soc. 131 (2009) 10368, doi:http://dx.doi.org/10.1021/ja9039983.
[12] C. Zhang, R.P. Lively, K. Zhang, J.R. Johnson, O. Karvan, W.J. Koros, J. Phys. Chem. Lett. 3 (2012) 2130, doi:http://dx.doi.org/10.1021/jz300855a.
[13] A.J. Brown, N.A. Brunelli, K. Eum, F. Rashidi, J. Johnson, W.J. Koros, C.W. Jones, S. Nair, Science 345 (2014) 72, doi:http://dx.doi.org/10.1126/science.1251181.
[14] X. Ma, P. Kumar, N. Mittal, A. Khlyustova, P. Daoutidis, K.A. Mkhoyan, M. Tsapatsis, Science 361 (2018) 1008, doi:http://dx.doi.org/10.1126/science.aat4123.
[15] W. Li, P. Su, Z. Li, Z. Xu, F. Wang, H. Ou, J. Zhang, G. Zhang, E. Zeng, Nat. Commun. 8 (2017) 406, doi:http://dx.doi.org/10.1038/s41467-017-00544-1.
[16] H. Bux, A. Feldhoff, J. Cravillon, M. Wiebcke, Y.S. Li, J. Caro, Chem. Mater. 23 (2011) 2262, doi:http://dx.doi.org/10.1021/cm200555s.
[17] Y. Pan, Z. Lai, Chem. Commun. 47 (2011) 10275, doi:http://dx.doi.org/10.1039/C1CC14051E.
[18] H.T. Kwon, H.K. Jeong, Chem. Commun. 49 (2013) 3854, doi:http://dx.doi.org/10.1039/c3cc41039k.
[19] M.C. Lovallo, A. Gouzinis, M. Tsapatsis, AIChE J. 44 (1998) 1903, doi:http://dx.doi.org/10.1002/aic.690440820.
[20] M.R.A. Hamid, H.K. Jeong, Korean J. Chem. Eng. 35 (2018) 1577, doi:http://dx.doi.org/10.1007/s11814-018-0081-1.
[21] D. Li, R. Wang, T.S. Chung, Sep. Purif. Technol. 40 (2004) 15, doi:http://dx.doi.org/10.1016/j.seppur.2003.12.019.
[22] F. Cacho-Bailo, S. Catalan-Aguirre, M. Etxeberria-Benavides, O. Karvan, V. Sebastian, C. Tellez, J. Coronas, J. Membr. Sci. 476 (2015) 277, doi:http://dx.doi.org/10.1016/j.memsci.2014.11.016.
[23] J. Ji, F. Liu, N.A. Hashim, M.R.M. Abed, K. Li, React. Funct. Polym. 86 (2015) 134, doi:http://dx.doi.org/10.1016/j.reactfunctpolym.2014.09.023.
[24] F. Liu, N.A. Hashim, Y. Liu, M.M. Abed, K. Li, J. Membr. Sci. 375 (2011) 1, doi:http://dx.doi.org/10.1016/j.memsci.2011.03.014.
[25] C. Zhang, B.H. Wu, M.Q. Ma, Z. Wang, Z.K. Xu, Chem. Soc. Rev. 48 (2019) 3811, doi:http://dx.doi.org/10.1039/C9CS00322C.
[26] J. Hou, P.D. Sutrisna, Y. Zhang, V. Chen, Angew. Chem. Int. Ed 55 (2016) 3947, doi:http://dx.doi.org/10.1002/anie.201511340.
[27] W. Li, Q. Meng, C. Zhang, G. Zhang, Chem.: Eur. J 21 (2015) 7224, doi:http://dx.doi.org/10.1002/chem.201500007.
[28] J. Hou, P.D. Sutrisna, T. Wang, S. Gao, Q. Li, C. Zhou, S. Sun, H.C. Yang, F. Wei, M.T. Ruggiero, ACS Appl. Mater. Interfaces 11 (2019) 5570, doi:http://dx.doi.org/10.1021/acsami.8b20570.
[29] W. Li, W. Wu, Z. Li, J. Shi, Y. Xia, J. Mater. Chem. A 6 (2018) 16333, doi:http://dx.doi.org/10.1039/C8TA06083E.
[30] M.R.A. Hamid, S. Park, J.S. Kim, Y.M. Lee, H.K. Jeong, Ind. Eng. Chem. Res. 58 (2019) 14947, doi:http://dx.doi.org/10.1021/acs.iecr.9b02969.
[31] M.J. Lee, M.R.A. Hamid, J. Lee, J.S. Kim, Y.M. Lee, H.K. Jeong, J. Membr. Sci. 559 (2018) 28, doi:http://dx.doi.org/10.1016/j.memsci.2018.04.041.
[32] M.R.A. Hamid, S. Park, J.S. Kim, Y.M. Lee, H.K. Jeong, J. Mater. Chem. A 7 (2019) 9680, doi:http://dx.doi.org/10.1039/C9TA00837C.
[33] S. Wongchitphimon, R. Wang, R. Jiraratananon, J. Membr. Sci. 381 (2011) 183, doi:http://dx.doi.org/10.1016/j.memsci.2011.07.022.
[34] X. Jiang, S. Li, Y. Bai, L. Shao, J. Mater. Chem. A 7 (2019) 10898, doi:http://dx.doi.org/10.1039/C8TA11748A.
[35] A. Huang, Q. Liu, N. Wang, J. Caro, J. Mater. Chem. A 2 (2014) 8246, doi:http://dx.doi.org/10.1039/C4TA00299G.
[36] Z. Yu, Y. Pan, Y. He, G. Zeng, H. Shi, H. Di, RSC Adv. 5 (2015) 51364, doi:http://dx.doi.org/10.1039/C5RA04894J.
[37] D. Brewis, I. Mathieson, I. Sutherland, R. Cayless, R. Dahm, Int. J. Adhes. Adhes. 16 (1996) 87, doi:http://dx.doi.org/10.1016/0143-7496(95)00053-4.
[38] A. Bottino, G. Capannelli, O. Monticelli, P. Piaggio, J. Membr. Sci. 166 (2000) 23, doi:http://dx.doi.org/10.1016/S0376-7388(99)00253-7.
[39] N. Meng, R.C.E. Priestley, Y. Zhang, H. Wang, X. Zhang, J. Membr. Sci. 501 (2016) 169, doi:http://dx.doi.org/10.1016/j.memsci.2015.12.004.
[40] L. Xiao, D.M. Davenport, L. Ormsbee, D. Bhattacharyya, Ind. Eng. Chem. Res. 54 (2015) 4174, doi:http://dx.doi.org/10.1021/ie504149t.
[41] M.E. Casco, Y.Q. Cheng, L.L. Daemen, D. Fairen-Jimenez, E.V. Ramos-Fernández, A.J. Ramírez-Cuesta, J. Silvestre-Albero, Chem. Commun. 52 (2016) 3639, doi:http://dx.doi.org/10.1039/C5CC10222G.
[42] H. Bux, F. Liang, Y. Li, J. Cravillon, M. Wiebcke, J.R. Caro, J. Am. Chem. Soc. 131 (2009) 16000, doi:http://dx.doi.org/10.1021/ja907359t.
[43] X. Wang, M. Sun, B. Meng, X. Tan, J. Liu, S. Wang, S. Liu, Chem. Commun. 52 (2016) 13448, doi:http://dx.doi.org/10.1039/C6CC06589A.
[44] K. Tao, L. Cao, Y. Lin, C. Kong, L. Chen, J. Mater. Chem. A 1 (2013) 13046, doi:http://dx.doi.org/10.1039/C3TA13371K.

[45] K. Tao, C. Kong, L. Chen, Chem. Eng. J. 220 (2013) 1, doi:http://dx.doi.org/10.1016/j.cej.2013.01.051.
[46] K. Huang, Z. Dong, Q. Li, W. Jin, Chem. Commun. 49 (2013) 10326, doi:http://dx.doi.org/10.1039/C3CC46244G.
[47] Y. Li, C. Ma, P. Nian, H. Liu, X. Zhang, J. Membr. Sci. 581 (2019) 344, doi:http://dx.doi.org/10.1016/j.memsci.2019.03.069.
[48] Q. Liu, N. Wang, J.R. Caro, A. Huang, J. Am. Chem. Soc. 135 (2013) 17679, doi:http://dx.doi.org/10.1021/ja4080562.
[49] J. Li, W. Cao, Y. Mao, Y. Ying, L. Sun, X. Peng, CrystEngComm 16 (2014) 9788, doi:http://dx.doi.org/10.1039/C4CE01503G.
[50] E. Shamsaei, X. Lin, Z.X. Low, Z. Abbasi, Y. Hu, J.Z. Liu, H. Wang, ACS Appl. Mater. Interfaces 8 (2016) 6236, doi:http://dx.doi.org/10.1021/acsami.5b12684.
[51] R. Wei, H.Y. Chi, X. Li, D. Lu, Y. Wan, C.W. Yang, Z. Lai, Adv. Funct. Mater (2019) 1907089, doi:http://dx.doi.org/10.1002/adfm.201907089.
[52] K. Huang, B. Wang, Y. Chi, K. Li, Adv. Mater. Interfaces 5 (2018) 1800287, doi:http://dx.doi.org/10.1002/admi.201800287.
[53] S. Zhou, Y. Wei, L. Li, Y. Duan, Q. Hou, L. Zhang, L.X. Ding, J. Xue, H. Wang, J. Caro, Sci. Adv. 4 (2018) 1393, doi:http://dx.doi.org/10.1126/sciadv.aau1393.
[54] H.T. Kwon, H.K. Jeong, A.S. Lee, H.S. An, J.S. Lee, J. Am. Chem. Soc. 137 (2015) 12304, doi:http://dx.doi.org/10.1021/jacs.5b06730.
[55] M.J. Lee, H.T. Kwon, H.K. Jeong, J. Membr. Sci. 529 (2017) 105, doi:http://dx.doi.org/10.1016/j.memsci.2016.12.068.
[56] C. Chen, A. Ozcan, A.O. Yazaydin, B.P. Ladewig, J. Membr. Sci. 575 (2019) 209, doi:http://dx.doi.org/10.1016/j.memsci.2019.01.027.
[57] L. Sheng, C. Wang, F. Yang, L. Xiang, X. Huang, J. Yu, L. Zhang, Y. Pan, Y. Li, Chem. Commun. 53 (2017) 7760, doi:http://dx.doi.org/10.1039/C7CC03887A.
[58] J. Li, H. Lian, K. Wei, E. Song, Y. Pan, W. Xing, J. Membr. Sci. 595 (2020) 117503, doi:http://dx.doi.org/10.1016/j.memsci.2019.117503.
[59] N.T. Tran, J. Kim, M.R. Othman, Sep. Purif. Technol. 233 (2020) 116026, doi:http://dx.doi.org/10.1016/j.seppur.2019.116026.
[60] J.B. James, L. Lang, L. Meng, J.Y.S. Lin, ACS Appl. Mater. Interfaces 12 (2020) 3893, doi:http://dx.doi.org/10.1021/acsami.9b19964.
[61] N.T. Tran, J. Kim, M.R. Othman, Microporous Mesoporous Mater. 285 (2019) 178, doi:http://dx.doi.org/10.1016/j.micromeso.2019.05.010.
[62] G. He, M. Dakhchoune, J. Zhao, S. Huang, K.V. Agrawal, Adv. Funct. Mater. 28 (2018) 1707427, doi:http://dx.doi.org/10.1002/adfm.201707427.
[63] F. Hillman, J.M. Zimmerman, S.M. Paek, M.R.A. Hamid, W.T. Lim, H.K. Jeong, J. Mater. Chem. A 5 (2017) 6090, doi:http://dx.doi.org/10.1039/C6TA11170J.
[64] M.J. Lee, H.T. Kwon, H.K. Jeong, Angew. Chem. Int. Ed 57 (2018) 156, doi:http://dx.doi.org/10.1002/anie.201708924.
[65] H.T. Kwon, H.K. Jeong, J. Am. Chem. Soc. 135 (2013) 10763, doi:http://dx.doi.org/10.1021/ja403849c.
[66] J.H. Lee, D. Kim, H. Shin, S.J. Yoo, H.T. Kwon, J. Kim, J. Ind. Eng. Chem. 72 (2019) 374, doi:http://dx.doi.org/10.1016/j.jiec.2018.12.039.
[67] C. Wang, F. Yang, L. Sheng, J. Yu, K. Yao, L. Zhang, Y. Pan, Chem. Commun. 52 (2016) 12578, doi:http://dx.doi.org/10.1039/C6CC06457D.
[68] Y. Pan, T. Li, G. Lestari, Z. Lai, J. Membr. Sci. 390 (2012) 93, doi:http://dx.doi.org/10.1016/j.memsci.2011.11.024.
[69] D. Liu, X. Ma, H. Xi, Y.S. Lin, J. Membr. Sci. 451 (2014) 85, doi:http://dx.doi.org/10.1016/j.memsci.2013.09.029.
[70] Y. Pan, W. Liu, Y. Zhao, C. Wang, Z. Lai, J. Membr. Sci. 493 (2015) 88, doi:http://dx.doi.org/10.1016/j.memsci.2015.06.019.
[71] J. Hao, D.J. Babu, Q. Liu, H.Y. Chi, C. Lu, Y. Liu, K.V. Agrawal, J. Mater. Chem. A (2020), doi:http://dx.doi.org/10.1039/C9TA12027K.
[72] S. Tanaka, K. Okubo, K. Kida, M. Sugita, T. Takewaki, J. Membr. Sci. 544 (2017) 306, doi:http://dx.doi.org/10.1016/j.memsci.2017.09.037.
[73] N. Hara, M. Yoshimune, H. Negishi, K. Haraya, S. Hara, T. Yamaguchi, J. Membr. Sci. 450 (2014) 215, doi:http://dx.doi.org/10.1016/j.memsci.2013.09.012.
[74] N. Hara, M. Yoshimune, H. Negishi, K. Haraya, S. Hara, T. Yamaguchi, Microporous Mesoporous Mater 206 (2015) 75, doi:http://dx.doi.org/10.1016/j.micromeso.2014.12.018.
[75] E. Barankova, X. Tan, L.F. Villalobos, E. Litwiller, K.V. Peinemann, Angew. Chem. Int. Ed. 56 (2017) 2965, doi:http://dx.doi.org/10.1002/anie.201611927.
[76] K. Eum, C. Ma, A. Rownaghi, C.W. Jones, S. Nair, ACS Appl. Mater. Interfaces 8 (2016) 25337, doi:http://dx.doi.org/10.1021/acsami.6b08801.
[77] K. Eum, A. Rownaghi, D. Choi, R.R. Bhave, C.W. Jones, S. Nair, Adv. Funct. Mater. 26 (2016) 5011, doi:http://dx.doi.org/10.1002/adfm.201601550.
[78] J.M.S. Henis, M.K. Tripodi, U.S. Patent, US4230463A, (1980) .
[79] E.A. Grushevenko, I.L. Borisov, A.A. Knyazeva, V.V. Volkov, A.V. Volkov, Sep. Purif. Technol. 241 (2020) 116696, doi:http://dx.doi.org/10.1016/j.seppur.2020.116696.
[80] X. Gong, S. He, ACS Omega 5 (2020) 4100, doi:http://dx.doi.org/10.1021/acsomega.9b03775.
[81] J. Peng, X. Zhao, W. Wang, X. Gong, Langmuir 35 (2019) 8404, doi:http://dx.doi.org/10.1021/acs.langmuir.9b01507.
[82] Y. Wang, X. Gong, Adv. Mater. Interfaces 4 (2017) 1700190, doi:http://dx.doi.org/10.1002/admi.201700190.
[83] L. Zhong, X. Gong, Soft Matter 15 (2019) 9500, doi:http://dx.doi.org/10.1039/C9SM01624D.
[84] X. Gong, J. Zhang, S. Jiang, Chem. Commun. 56 (2020) 3054, doi:http://dx.doi.org/10.1039/C9CC08768K.
[85] M. Galizia, W.S. Chi, Z.P. Smith, T.C. Merkel, R.W. Baker, B.D. Freeman, Macromolecules 50 (2017) 7809, doi:http://dx.doi.org/10.1021/acs.macromol.7b01718.